Journal of Materials Chemistry

Cite this: J. Mater. Chem., 2011, 21, 13769

www.rsc.org/materials

COMMUNICATION

Acicular nanoparticles formed through coprecipitation of iron salts in the presence of bovine serum albumin†

Martin J. Hadley,[a] Adrian J. Wright,[b] Neil A. Rowson[a] and Liam M. Grover*[a]

Received 27th May 2011, Accepted 14th July 2011
DOI: 10.1039/c1jm12387d

Coprecipitation of ferric and ferrous iron salts in the presence of Bovine Serum Albumin (BSA) demonstrates an unusual impact on crystal growth mechanisms and eventual nanoparticle morphology. For BSA 200–800μMol/ml, polycrystalline acicular and haloed spheroid particles were observed and these samples demonstrated surprising magnetic properties, including high coercivity.

Iron oxide demonstrates a unique ubiquity in geology, biology and industrial application due in no small part to the common spinel ferrite structure $M \cdot Fe_2O_4$.[1] Biomineralisation and various wet chemical or emulsion techniques are able to impose a high degree of crystal growth and morphological regulation. In nature, magnetic nanoparticles (MNPs) are observed within bacteria,[2] birds[3] as well as other species and are believed to be involved in magnetoreception.[4] Coprecipitation of iron salts is widely regarded as the least energy intensive and easiest means to manipulate the synthesis of MNPs. However, the ability to selectively change crystal growth to achieve industrially useful secondary structures has proved difficult by precipitation alone. Acicular MNPs with high coercivity have potential applications in biomedicine and high density magnetic storage devices, but are particularly difficult to obtain by coprecipitation as the overgrowth of Fe_3O_4 away from the preferred spherical shape is thermodynamically unfavoured.[5,6]

Biomineralisation is largely dependent on encouraging preferential crystal growth away from geologically-derived forms and this requires careful manipulation of the free-energy and enthalpy landscape to select otherwise unstable polymorphs,[7] or alternative morphologies. In a landmark paper Belcher *et al.*[8] demonstrated that complex pre-organised organic arrays were not necessarily required for polymorph selection, soluble proteins extracted from aragonitic and calcitic portions of mollusc shell were sufficient to preferentially select that crystal growth pathway. Recently, attempts to replicate the complex MNPs observed in magnetotactic bacteria by soluble magnetosome-derived protein alone have been made with relative success.[9]

Much work has been published recently concerning protein separation by adsorption and later desorption on to MNPs has been demonstrated with particular emphasis on the model protein, bovine serum albumin (BSA).[10] BSA has a high iron binding potential and is capable of adsorbing 8.5 moles of iron per mole of protein,[11] although contrary statements are found in the literature[12] it is generally accepted that BSA possesses a ligand with particular preference for ferric iron (Fe^{3+}).[13]

We demonstrate in this communication the coprecipitation of ferrous sulphate and ferric chloride (2mMol/ml and 1.3mMol/ml, respectively) in the presence of BSA (Sigma Aldrich A7906, ≥ 98% purity) over various concentrations from 0–1mMol/ml. In the absence of protein, black iron oxide material is immediately deposited upon the addition of sodium hydroxide. Transmission electron microscopy (TEM) identified two particle species: electron dense plate-like material and poorly formed particles less than 10nm in size.

Low protein concentration (9μMol/ml, ≤ 1% of bovine blood concentration[14]) rapidly decelerated deposition of iron oxide from the supernatant from instantaneous to several hours. At BSA concentrations in the range of 200–800μMol/ml full deposition took over 48h, however atomic absorption spectroscopy (AAS) indicated continued removal of iron from the supernatant which suggests a mass limited transport mechanism for iron oxide precipitation within the samples - although within 7 days 90% of iron had been removed from the supernatant. High protein concentration (≥ 800μMol/ml) entirely prevented deposition of material from the supernatant, after addition of sodium hydroxide these samples appear straw coloured before darkening to jet black after 7 days and remaining stable over 6 weeks. In the case of BSA 200–800μMol/ml a complex precipitate evolution was observed by TEM, as demonstrated in Fig. 1. The observation of protein inhibiting, or decelerating mineralisation in both biological and artificial systems has been widely reported with particular attention demonstrated in the tissue engineering field.[15]

When imaged at 24 and 48h, large scale fractal-like structures (≤ 100μm) are clearly observed - as shown for 270μMol/ml in Fig. 1. These structures are clearly non-crystalline with some small electron-dense features thinly distributed internally (large axis ≤ 100nm). We propose these are globularised protein networks within which iron oxide material is maturing. It remains unclear why these structures dissipate within 72h and why these structures appear to be size limited. We would expect a sample

[a]Chemical Engineering, University of Birmingham, Edgbaston, B15 2TT, UK. E-mail: l.m.grover@bham.ac.uk; Tel: (+44) (0) 121 414 3887
[b]Chemistry, University of Birmingham, Edgbaston, B15 2TT, UK
† Electronic Supplementary Information (ESI) available: Experimental details. See DOI: 10.1039/c1jm12387d

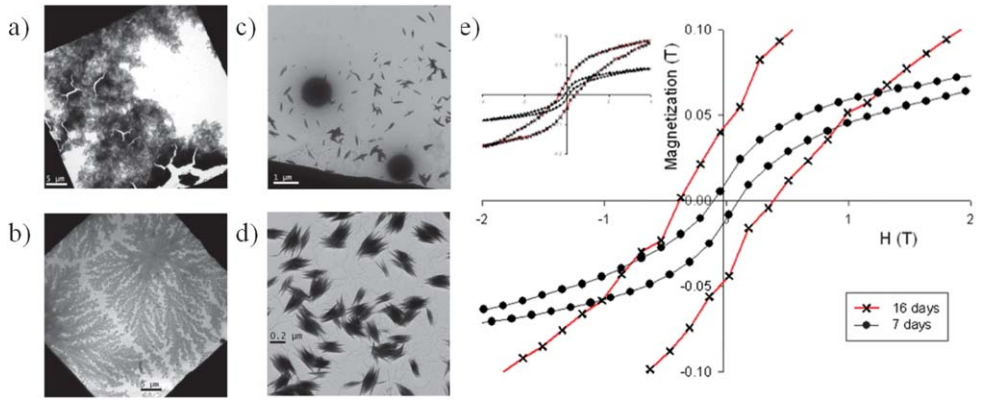

Fig. 1 TEM images and hysteresis loop. *a*) Control after 24 h, *b*) BSA 270μMol/ml after 24 h, *c*) BSA 495μMol/ml after 7 days, *d*) BSA 495μMol/ml after 6 weeks, and *e*) hysteresis loops for BSA 495μMol/ml showing characteristic changes in coercive field and remanence of the precipitated material over time (from day 7 to day 16) - 0.10T to 0.38T and 0.012T to 0.044T, inset: complete hysteresis loops.

wide protein network, however distinct fractal structures are clearly evident.

All samples in the BSA 200–800μMol/ml range demonstrated polycrystalline acicular particles with aspect ratios of 4 and a maximum extension of 700nm, as well as haloed spheroid particles of diameter 1μm. These structures were particularly prevalent for BSA 495μMol/ml and as such our results focus on these samples. Particular attention is brought to the polycrystalline acicular particles, the formation mechanism of which is currently not understood. We propose two possible growth pathways: exclusively diffusion-limited nucleation within the transient proteinaceous network demonstrated in Fig. 1 or else preferential protein adsorption to the elongated axis (assumed [111][16]) of diffusion-limited prenucleation clusters within the network. The two highlighted particular species appear entirely distinct, the haloed spheroids do not appear to be crystalline in nature and demonstrate limited degradation within the TEM electron beam, whereas the acicular nanoparticles clearly demonstrate a polycrystalline structure (see Fig. 1)

In all samples that demonstrated eventual deposition of material (BSA 0–800μMol/ml) gentle agitation was sufficient to fully disperse all precipitated material. The application of a barium ferrite magnet successfully collected all material to the sample container edge, further agitation was sufficient to redisperse the precipitated material. Vibrating sample magnetometry (VSM) indicated surprisingly high coercivity and remanence, data for BSA 495μMol/ml is shown in Fig. 1. Time-lapsed measurements show sample maturity further improves these values, from day 7 to 16 the coercivity and remanence increased markedly from 0.10T to 0.38T and 0.012T to 0.044T, respectively. The coercive field is quite large compared to that found elsewhere in the literature, for example Wiogo *et al.*[17] report highly crystalline nanobelts with high aspect ratios ($\leq$ 40) and a coercive field of $\sim$0.02T, an alternative one-step wet chemical method for high aspect ratio ($\leq$ 20) aciciular MNPs developed by Chen *et al.*[5] yields similar coercive fields. TEM indicated that the haloed spheroid particles remain unchanged over several weeks, however the polycrystalline acicular nanocrystals preferentially align and aggregate along the long axis, we include images after 6 weeks in Fig. 1 to emphasise this.

It is thus tempting to implicate the acicular particle aggregation and increasing electron density in the improving magnetic properties, and further more to consider them as acicular iron oxide

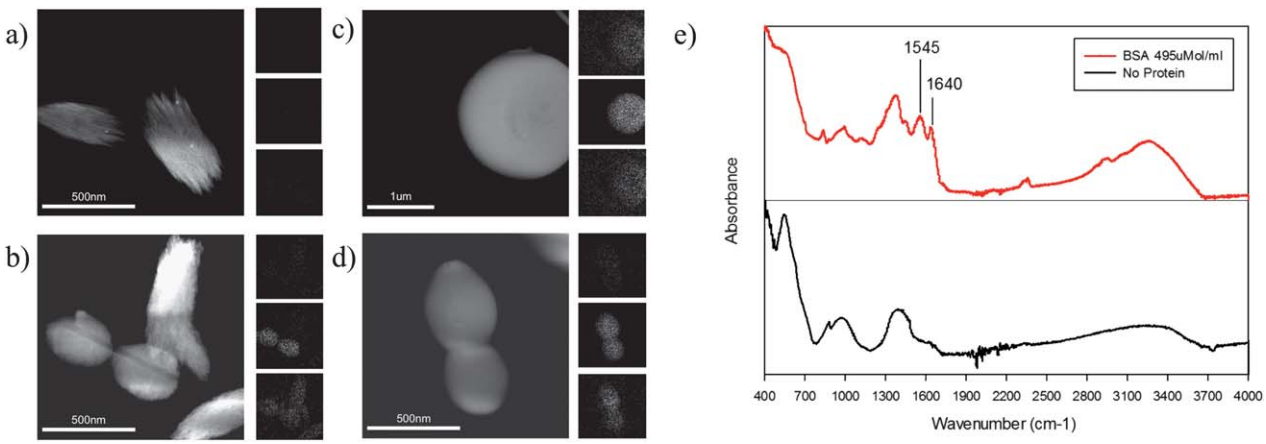

Fig. 2 STEM images with EDX element maps, from top to bottom; iron, sulphur, oxygen. *a-b*) Acicular nanoparticles imaged after 7 and 14 days, respectively, *c-d*) haloed spheroid particles imaged after 7 and 14 days, respectively, *e*) normalised FTIR spectra for precipitate formed both in the presence (red) and absence of protein (black).

nanoparticles of the spinel ferrite structure. However, energy dispersive X-ray spectroscopy (EDX) indicates a much lower iron content than would be expected if these particles were entirely formed of iron oxide, Fig. 2. Spectra from EDX (data not shown) indicates iron is present in all particles included in Fig. 2, however the oxygen and sodium content of each particle was much higher than expected. The material precipitated in the presence of BSA 200–800μMol/ml clearly demonstrates protein inclusion from Fourier Transform Infra-Red (FTIR) spectroscopy. Fig. 2 includes such a spectra for BSA 495μMol/ml, demonstrating distinct peaks at 1545 and 1640cm^{-1} similar to those reported previously for BSA[10,18] and attributable to Amide II and Amide I respectively,[19] these peaks are not observed in the absence of protein. Attributing sulphur to cysteine in BSA (see Fig. 2), the haloed spheroids are identified as protein globules and we also note the apparent low protein concentration in the acicular particles. Despite the low iron content of both particle species, we argue that their physical and population size are sufficient for their deposition to be noticeable if they were not subject to attraction to the applied magnetic field from barium ferrite material, and this was not observed.

In conclusion, we have demonstrated that the coprecipitation of iron salts in the presence of BSA radically decelerates iron oxide precipitation and over the concentration range 200–800μMol/ml results in the formation of haloed spheroid particles and poly-crystalline acicular particles after 72h ageing *in situ*. While the haloed spheroids remain essentially stable over 6 weeks, the acicular particles aggregate preferentially along the long axis. Hysteresis data suggests high coercive and remanence fields for BSA 495μMol/ml that increase over time, while this is assumed to be due to the acicular nanoparticles both possessing a spinel ferrite structure and their observed aggregation this has not yet been fully proven.

Acknowledgements

This project was funded by the Biotechnology and Biological Sciences Research Council (BBSRC).

References

1 R. S. Tebble and D. J. Craik, *Magnetic Materials*, Wiley-Interscience, London, 1969.
2 S. Staniland, B. Ward, A. Harrison, G. van der Laan and N. Telling, *Proc. Natl. Acad. Sci. U. S. A.*, 2007, **104**, 19524–8.
3 G. Falkenberg, G. Fleissner, K. Schuchardt, M. Kuehbacher, P. Thalau, H. Mouritsen, D. Heyers, G. Wellenreuther and G. Fleissner, *PLoS One*, 2010, **5**, e9231.
4 J. L. Gould, *Curr. Biol.*, 2008, **18**, R482–4.
5 S. Chen, J. Feng, X. Guo, J. Hong and W. Ding, *Mater. Lett.*, 2005, **59**, 985–988.
6 H. Wiogo, M. Lim and R. Amal, *Chemeca 2008: Towards a Sustainable Australasia*, 2008, pp. 1848–1858.
7 S. Raz, S. Weiner and L. Addadi, *Adv. Mater.*, 2000, **12**, 38–42.
8 A. M. Belcher, X. H. Wu, R. J. Christensen, P. K. Hansma, G. D. Stucky and D. E. Morse, *Nature*, 1996, **381**, 56–58.
9 C. Arakaki, J. Webb and T. Matsunaga, *J. Biol. Chem.*, 2003, **278**, 8745–50.
10 Z. G. Peng, K. Hidajat and M. S. Uddin, *J. Colloid Interface Sci.*, 2004, **271**, 277–83.
11 A. Loban, R. Kime and H. Powers, *Clinical Science*, 1997, **95**, 445–451.
12 K. J. Collard, *Pediatrics*, 2009, **123**, 1208–16.
13 R. C. Hider, *Eur. J. Clin. Invest.*, 2002, **32**(Suppl. 1), 50–4.
14 S. Fernandez, J. Rodriguez and a. Padilla, *Desalination*, 1999, **126**, 95–100.
15 C. Combes and C. Rey, *Biomaterials*, 2002, **23**, 2817–23.
16 C. Jimenez-Lopez, C. S. Romanek and D. a. Bazylinski, *J. Geophys. Res.*, 2010, **115**, 1–19.
17 H. Wiogo, M. Lim and P. Munroe, *Cryst. Growth Des.*, 2011, 1689–1696.
18 R. V. Mehta, R. V. Upadhyay, S. W. Charles and C. N. Ramchand, *Biotechnol. Tech.*, 1997, **11**, 493–496.
19 J. Kong, *Acta Biochim. Biophys. Sin.*, 2007, **39**, 549–559.